Lawrence Berkeley National Laboratory
Recent Work

Title
MICROSTRUCTURE AND MAGNETIC PROPERTIES OF Fe-Cr-Co ALLOYS

Permalink
https://escholarship.org/uc/item/4x5648kz

Author
Okada, M.

Publication Date
1978-02-01

UC-25

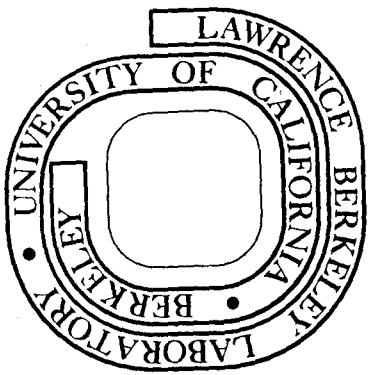# MICROSTRUCTURE AND MAGNETIC
PROPERTIES OF Fe-Cr-Co ALLOYS

M. Okada, G. Thomas, M. Homma, and
H. Kaneko

February 1978

DISCLAIMER

MICROSTRUCTURE AND MAGNETIC PROPERTIES OF Fe-Cr-Co ALLOYS[*]

M. Okada, G. Thomas, M. Homma,[†] and H. Kaneko[†]

Department of Materials Science and Engineering
College of Engineering and
Materials and Molecular Research Division
Lawrence Berkeley Laboratory
University of California
Berkeley, California 94720

ABSTRACT

The microstructures of an Fe-31wt%Cr-23wt%Co ductile permanent magnet alloy after isothermal aging, thermomagnetic treatment and step-aging have been characterized by transmission electron microscopy and by measurement of the Curie temperature. Isothermal aging itself produces the undesirable microstructure. Aging at 640°C develops the magnetic chromium-rich phase. Aging at 600°C produces a nonmagnetic chromium-rich phase dispersed within the iron-rich phase. The effect of thermomagnetic treatment on the microstructure of the alloy is discussed in comparison with that of Alnico alloys. Step-aging produces the desirable microstructure viz., elongated ferromagnetic phase imbedded in the paramagnetic phase.

INTRODUCTION

Fe-Cr-Co alloys are known to be potentially ductile hard magnets. These alloys were designed by following the miscibility gap in the Fe-Cr system into the Fe-Cr-Co ternary system.[1] The shape of the miscibility gap in the Fe-Cr-Co system is now well established.[2]

The magnetic hardening of the alloys is associated with decomposition within the miscibility gap producing modulated structures, consisting of two phases, an iron-rich phase (α_1) and a chromium-rich phase (α_2). The features of the decomposition are consistent with those expected from spinodal decomposition of the high temperature phase (α) during aging.[1],[3]

In order to control the magnetic properties of materials, it is important to characterize and control their microstructures. However, no systematic studies of the microstructure of these alloys have been reported. Thus the purpose of the present investigation is to establish some of the microstructure-property relationships in Fe-Cr-Co alloys resulting from a series of heat treatments (isothermal aging, thermomagnetic treatment, and step-aging). Since the microstructural changes occur on such a fine scale, transmission electron microscopy must be employed for characterization.[4]

EXPERIMENTAL PROCEDURES

An Fe-31wt%Cr-23wt%Co alloy was chosen for the present investigation because the decomposition tie line of the alloy is well established.[2]

The alloy was melted in an induction furnace from 99.9% electrolytic iron, 99.9% electrolytic chromium and 99.9% cobalt. Chemical analysis verified that the final alloy was within 1% of the desired composition. The ingot was then placed in a quartz tube, homogenized for one day at 1300°C and quenched into water. Slices, 0.5 mm thick, were cut and solution treated at 1300°C for 30 min under argon atmosphere in a vertical resistance furnace. Specimens were then quenched from 1300°C into iced brine at a rate of over 100°C/sec to avoid γ or σ phase formation.

The changes in microstructure, volume fraction of phases and wavelength (interrod spacing) were established by electron microscopy and diffraction, including high resolution lattice imaging, [4] and the utilization of laser optical diffraction.[5],[6] Electron microscopy disc specimens were thinned in an automatic jet polisher using an electrolytic solution of 23% perchloric acid and 77% acetic acid. The composition fluctuations were deduced by measuring the Curie temperature of the decomposed Cr-rich phase (α_2).[7] Since the Curie temperature of the α_1 phase is approximately 900°C,[8] measurements well below 900°C can be directly related to the composition of the α_2 phase. The magnetization as a function of temperature was measured with a magnetic balance while the specimen was heated at a rate of 10°C/min.

RESULTS

A.   Isothermal Aging

The series of bright field micrographs shown in Fig. 1 were taken

from the alloy aged for 1 hr at 680°C, 670°C, 660°C, and 650°C, respectively.

The phase with bright contrast is identified as the α_1 phase, the phase

with dark contrast as the α_2 phase. These micrographs reveal that the

miscibility gap of the alloy is below 670°C, and also show that the

morphology of the aged microstructure is very sensitive to the aging

temperature. At the lower aging temperatures the dispersion is finer

and the two phases more interconnected, and have rod-like shapes.

The microstructures shown in Fig. 2 were obtained from the alloy

aged at 640°C for 3 min, 20 min, 2 hr, and 20 hr. The decomposition process

appears to be isotropic in the alloy and is associated with halo-type

diffuse satellites in the corresponding diffraction pattern as shown in

Fig. 3. The radius of these diffuse satellites decreases with aging time

as the modulation wavelength increases. This behavior is typical of

spinodal coarsening.[7] After prolonged aging the α_1 phase becomes aligned

along the $\langle 100 \rangle$ directions as shown in Fig. 2(c),(d), and this produces

peaking along $\langle 100 \rangle$ in the diffraction pattern of Fig. 3(c),(d).

The micrographs shown in Fig. 4 are taken from the alloy aged at

600°C for 20 min, 2 hr, 100 hr, and 500 hr. The main difference in micro-

structures between Fig. 2 and Fig. 4 is that the α_2 phase is the major

phase in Fig. 2 and the minor one in Fig. 4. This can be understood from

the asymmetry in shape of the miscibility gap in the Fe-Cr-Co system.[2]

As the aging temperature is changed, different tie lines are encountered

and the volume fractions of α_1 and α_2 phases change. In the present alloy

equal fractions of the two phases would be obtained by aging near 635°C.
Thus small changes in aging temperature can produce large changes in
microstructural distributions of the α_1 and α_2 phases.

Figure 5(a) shows a high resolution (110) lattice image taken from
the alloy aged at 660°C for 1 hr [see Fig. 1(c)]. The (110) fringes
appear to be continuous across the interface between the α_1 and α_2 phases.
The difference in lattice parameters of the two phases was detected by
laser optical diffraction as shown in Fig. 5(b).[5] This experiment
provides direct evidence that both phases are coherent.

The magnetization as a function of temperature for the alloy aged
at 640°C is illustrated in Fig. 6. The magnetization of the specimens in
the as-quenched and aged state decreases with temperature up to approxi-
mately 400°C and then increases above 400°C and has a small peak. The
magnetization curve is found to be reversible up to 400°C, but irreversible
above 400°C, suggesting that the composition of the two phases does not
change during heating up to 400°C.

In Fig. 6, the magnetization curve of the specimen B aged at 640°C
for 20 min changes slope around 310°C, which is identified as the Curie
temperature of the α_2 phase.[2] The longer the aging time, the sharper
the discontinuity in the slope of this curve appears. The Curie temperature
of the α_2 phase aged at various temperatures as a function of aging time
is summarized in Fig. 7. These results suggest: 1) that the decomposed
phases reach their equilibrium composition within almost two hours;
2) that the α_2 phase developed during aging at 600°C is nonmagnetic at

room temperature, but is magnetic after aging at 640°C or 620°C. These results illustrate the sensitivity of the properties to aging temperature which means precipitate composition and morphology.

B.   Thermomagnetic Treatment

Thermomagnetic treatments play an important role in producing good magnetic properties. Figure 8 shows micrographs of the alloy aged at 640°C for 20 min, 1 hr, and 3 hr in a magnetic field of 2 kOe and their corresponding laser optical diffraction patterns. The bright field micrograph, Fig. 8(A), shows that the α_1 phase is oriented almost randomly. However, the corresponding laser optical diffraction, Fig. 8(a), exhibits peaked intensities (marked M), which implies some tendency for the α_1 phase to be aligned along this direction. The remanence in this state is nearly 0.6 I_s (I_s is the saturation magnetization).

Prolonged thermomagnetic aging causes the α_1 phase to be more elongated parallel to the direction marked M, as shown in Fig. 8(B),(C), and the corresponding laser optical diffraction patterns Fig. 8(b),(c). The remanence after magnetic-aging for 1 hr increases to almost 0.9 I_s. This remanence remains unchanged after step-aging. The high remanence indicates that the ferromagnetic α_1 phase is elongated along the direction of the applied magnetic field, independently of crystal orientation.[3] This stems from the fact that the decomposition process is found to be isotropic during the early stage of aging for at least 1 hr. The independence of the magnetic properties on the crystal orientation is already confirmed by the measurements of magnetic properties of single crystals of the alloy.[9]

When the thermomagnetic-aging time exceeds 2 hr, the remanence

decreases to about 0.8 I_s. This decrease can possibly be explained as follows. Under ideal circumstances, even after prolonged aging in a magnetic field, the α_1 phase would maintain its alignment parallel with the applied field. However, the present observation suggests that in fact the α_1 phase cannot maintain this alignment in certain localized areas such as that marked M in Fig. 9. It is believed that in these areas particle alignment is highly affected by the elastic constraints of the matrix, since elastic strain energy minimization favors a ⟨100⟩ particle growth direction. Therefore the exact direction of alignment within these regions is determined by a balance between the applied magnetic field and elastic strain field of the matrix. Therefore, the optimum time for the thermomagnetic treatment is limited from 40 min to 1 hr at 640°C. The field strength for the thermomagnetic treatment should be over 2 kOe. [10]

C.   Step-Aging

It is reported that step-aging has a beneficial effect not only on improving the magnetic properties of Fe-Cr-Co alloys, [1] but also on improving the mechanical properties of Cu-Ni-Fe alloys. [11] Figure 10(a) shows the microstructure taken from the alloy aged at 640°C for 40 min in a magnetic field of 2 kOe. The ferromagnetic phase is somewhat elongated along the direction of the magnetic field and has an interpenetrating rod-like morphology. The rod diameter is about 100 Å and the rod length 280 Å, giving a ratio of length to diameter of nearly 3.

Figure 10(b) shows the microstructure of the alloy given a thermomagnetic treatment at 640°C for 40 min and subsequently step-aged at 620°C for 20 min and at 600°C for 1 hr. Throughout step-aging it is found that

the ratio of length to diameter of the α_1 phase remains essentially
unchanged (130 Å in diameter, 370 Å in length), and that the volume
fraction of the α_1 phase increases slightly from 45% to 55%. The main
change during step-aging is that of composition of the two phases, which
is confirmed by the measurement of the Curie temperature of the α_2 phase
of the step-aged alloy.[2] The α_2 phase is magnetic at room temperature
just after the thermomagnetic treatment, but it becomes nonmagnetic
after step-aging. Therefore, the increase in coercivity during step-
aging is believed to be associated with a change in composition of
the two phases, resulting in an increase in the difference between the
magnetization intensities of the two phases.

DISCUSSION

The present microstructural observations are consistent
with the results of the reported miscibility gap in the Fe-Cr-Co system.[2]

The decomposition process of the alloy in the early stages of aging
appears to be isotropic. The direct evidence for this is the halo-type
diffuse satellites in the corresponding electron diffraction pattern
[Fig. 3(a)(b)] which can be reproduced by laser optical diffraction
[Fig. 8(a)]. The isotropic nature of the decomposition of the Fe-Cr-Co
alloy is very much different from the decomposition observed in Alnico
alloys, which tends to decompose along the (100) directions.[12],[13]
Thus the effect of thermomagnetic treatments on the microstructures of
these alloys must also be different. The ferromagnetic phase in Alnico
alloys preferentially grows along the (100) axis of each grain that is
closest to the magnetic field direction.[12] However, the α_1 phase in
Fe-Cr-Co alloys is elongated along the direction of the applied magnetic
field, independently of the crystal orientation of the grains.[3]

The properties of Alnico alloys can be further improved with an alloy
which has a (100) texture,[13] utilizing the anisotropic decomposition to
more efficiently elongate the ferromagnetic phase into the direction of
the applied magnetic field. The Fe-Cr-Co alloys are not improved by such
treatments.[9]

One possible method to improve the magnetic properties of Fe-Cr-Co
alloys should be that of adding those elements which make the decomposition
anisotropic, as Ti additions do in Alnico 9.[13] This means increasing the
elastic strain energy during decomposition. An example of such an element
in this system is reported to be Mo.[1],[14] Although the addition
of Mo to Fe-Cr-Co improves the magnetic properties,[1] it is not a

practically attractive method since Mo stimulates the formation of the embrittling σ phase. In order to further improve the magnetic properties while retaining good workability of the alloy, investigations of other quaternary alloying additions are clearly required. It is shown that isothermal aging itself fails to produce the optimum microstructure for good Fe-Cr-Co magnets. Aging at 640°C does not develop the nonmagnetic α_2 phase. Aging at 600°C also produces an undesirable microstructure because it results in the dispersion of the nonmagnetic α_2 phase within the α_1 phase. However, it is shown here that these problems can be overcome by step-aging, which gives a microstructure of elongated ferromagnetic α_1 phase imbedded in the paramagnetic α_2 phase.

It should be emphasized that this step-aging method to produce the desired microstructure is valid only when the step-aging temperature interval ($\Delta T = T_{\text{step n}} - T_{\text{step n-1}}$) is small. When the alloy is aged at low temperatures (580°C or 560°C) after thermomagnetic treatment ($\Delta T \geqslant 60°C$), secondary decomposition takes place as shown in Fig. 11. This secondary decomposition results in a deterioration of the magnetic properties of the alloy. A possible explanation of this may be that as the diameter of the decomposed phase is around 45 Å, this phase could behave as a superparamagnetic domain.[15]

CONCLUSION

The microstructures of an Fe-31wt%Cr-23wt%Co permanent magnet alloy after isothermal aging, thermomagnetic treatment and step-aging have been studied in connection with their magnetic properties. The morphology of the microstructure is very sensitive to the aging temperature. The volume fraction of the two phases varies with aging temperature. The decomposition process appears to be isotropic, being associated with halo-type diffuse satellites in the diffraction pattern. Continued aging develops a periodically modulated structure along $\langle 100 \rangle$. The lattice imaging technique reveals that the two phases are coherent. Curie temperature measurements show that decomposed phases reach their equilibrium composition after about two hours aging. Isothermal aging itself produces undesirable microstructures. Aging at 640°C develops the magnetic Cr-rich phase. Aging at 600°C produces a nonmagnetic Cr-rich phase dispersed within the Fe-rich phase. The optimum thermomagnetic treatment of the alloy involves aging at 640°C for 40 min to 1 hr in a magnetic field of 2 kOe. The ferromagnetic phase is then elongated along the direction of the applied magnetic field, independent of crystal orientation. Step-aging produces a beneficial microstructure, viz., the elongated ferro-magnetic α_1 phase imbedded in the paramagnetic α_2 phase. The increase in coercivity by step-aging is found to be associated with a change in composition of the two decomposed phases, the morphology of the iron-rich phase remaining unchanged.
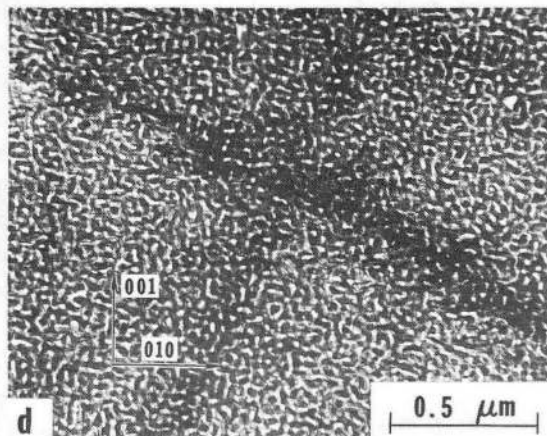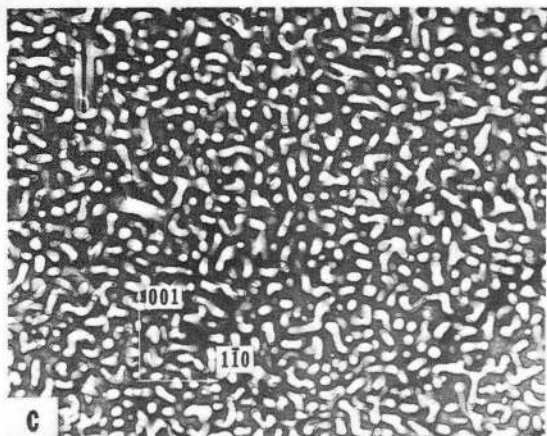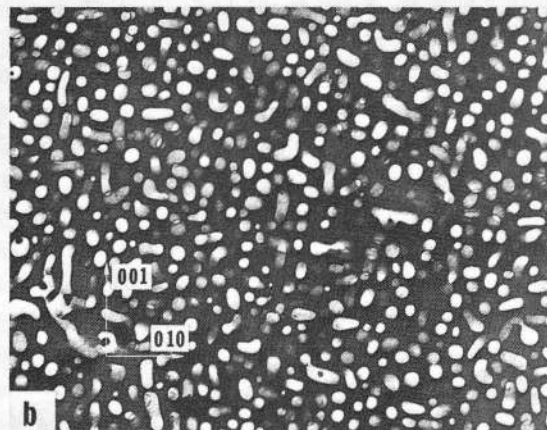
REFERENCES

(1)   H. Kaneko, M. Homma and K. Nakamura, "New Ductile Permanent Magnet
       of Fe-Cr-Co System," AIP Conf. Proc., No. 5, p.1088 (1971).

(2)   H. Kaneko, M. Homma, K. Nakamura, M. Okada and G. Thomas, "Phase
       Diagram of Fe-Cr-Co Permanent Magnet System," IEEE Proc. on
       Magnetics (September 1977).

(3)   M. Okada, M. Homma, H. Kaneko and G. Thomas, "The Microstructure
       of Fe-Cr-Co-Nb-Al Permanent Magnet," 34th Ann. Proc. EMSA, p.606 (1976).

(4)   G. Thomas, "High Voltage and High Resolution Electron Microscopy
       in Materials Science," J. of Metals, Vol. 29, No. 2, p.31 (1977).

(5)   R. Sinclair, R. Gronsky and G. Thomas, "Optical Diffraction from
       Lattice Images of Alloys," Acta Met., Vol. 24, p.789 (1976).

(6)   D. R. Clarke, "The Optical Reflection Transform Method,"
       J. of Mater. Sci., Vol. 10, p.172 (1975).

(7)   E. P. Butler and G. Thomas, "Structure and Properties of Spinodally
       Decomposed Cu-Ni-Fe Alloys," Acta Met., Vol. 18, p.347 (1970).

(8)   M. Hansen, "Constitution of Binary Alloys," 2nd edition, p.472
       (McGraw-Hill, 1958).

(9)   H. Kaneko, M. Homma, M. Okada, S. Nakamura and N. Ikuta, "Fe-Cr-Co
       Ductile Magnet with $(BH)_{max} \simeq 8$ MGOe," AIP Conf. Proc., No. 29,
       p.620 (1975).

(10)   H. Kaneko, M. Homma and K. Nakamura, (unpublished work).

(11)   K. Kubarych, M. Okada and G. Thomas, "Improvement of the Mechanical
       Properties of Spinodal Cu-Ni-Fe Alloys by Nonconventional Heat
       Treatment," presented in Fall AIME Meeting (1976), to be published.

-13-

(12)   R. D. Heidenreich and E. A. Nesbitt, "Physical Structure and

Magnetic Anisotropy of Alnico 5," J. Appl. Phys., Vol. 23,

p.352 (1952).

(13)   K. J. De Vos, "Alnico Permanent Magnet Materials," Vol. 1,

Magnetism and Metallurgy, p.473 (Academic Press, 1969).

(14)   R. Cremer and I. Pfeiffer, "Permanent Magnet Properties of Cr-Co-Fe

Alloys," Physica, Vol. 80B, p.164 (1975).

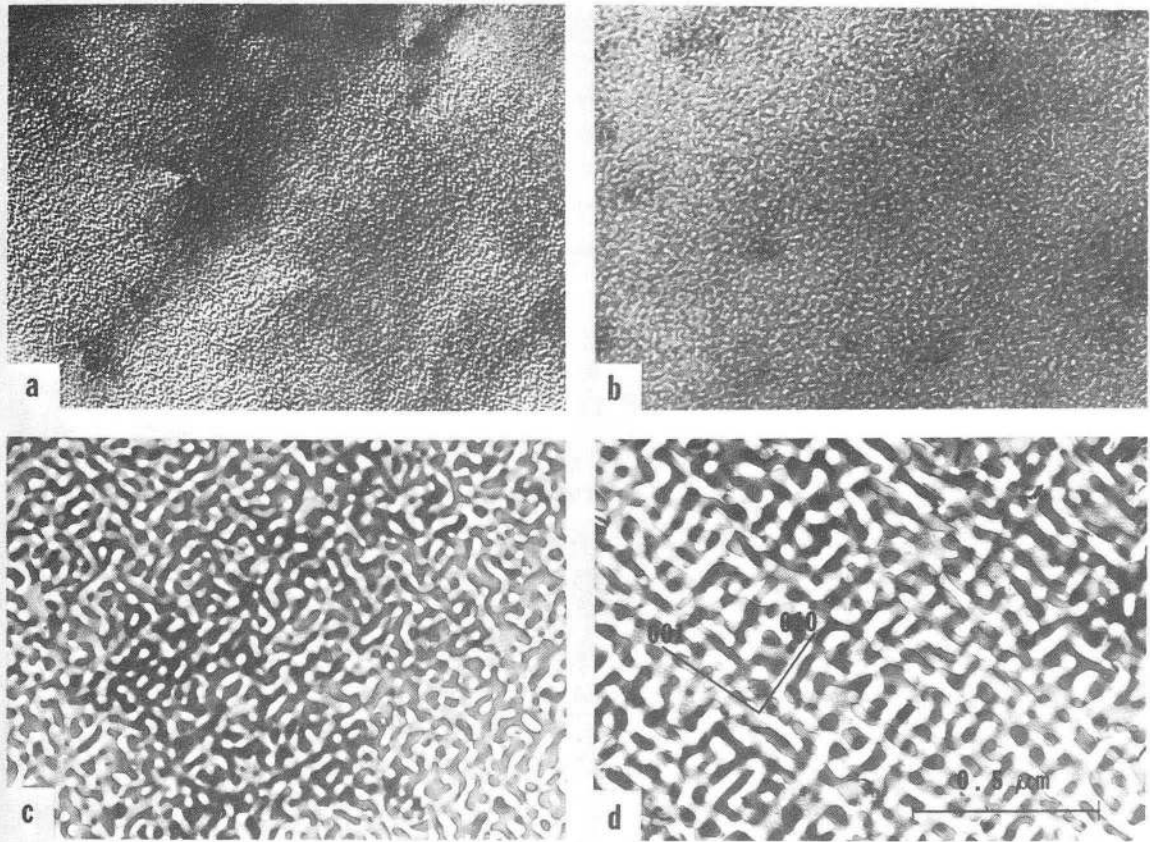(15)   C. P. Bean and J. D. Livingston, "Superparamagnetism," J. Appl.

Phys., Vol. 30, 120S (1959).

FIGURE CAPTIONS

Fig. 1.   Bright field micrographs of the Fe-31wt%Cr-23wt%Co alloy aged for

1 hr at (a) 680°C, (b) 670°C, (c) 660°C, and (d) 650°C.

Fig. 2.   Bright field micrographs of the alloy at 640°C for (a) 3 min,

(b) 20 min Hc~100 Oe, (c) 2 hr Hc~160 Oe, (d) 20 hr Hc~125 Oe.

Fig. 3.   Satellites around (002) reflections in the corresponding diffraction

patterns of Fig. 1.

Fig. 4.   Micrographs of the alloy aged at 600°C for (a) 20 min Hc~15 Oe,

(b) 2 hr Hc~35 Oe, (c) 100 hr Hc~200 Oe, (d) 500 hr Hc~260 Oe.

Fig. 5.   (110) lattice image (a) and corresponding laser optical diffraction

pattern (b) of the alloy aged at 660°C for 1 hr.

Fig. 6.   The magnetization as a function of temperature of the alloy

aged at 640°C.

Fig. 7.   Curie temperatures of the Cr-rich phase aged at various temperatures

as a function of aging time.

Fig. 8.   Bright field micrographs of the alloy aged at 640°C in a magnetic

field of 2 KOe for (A) 20 min, (B) 1 hr, and (C) 3 hr, and their

corresponding laser optical diffraction patterns (a), (b), and (c).

Fig. 9.   Bright field micrograph taken from the alloy magnetically-aged

at 640°C for 3 hr, localized deviation in particle alignment is

shown at M.

Fig. 10. (a) Micrograph of the alloy aged at 640°C for 40 min in a

magnetic field of 2 KOe, Hc~130 Oe.   (b) Micrograph of the

alloy step-aged at 620°C for 20 min and 600°C for 1 hr after

thermomagnetic treatment, Hc~410 Oe.

Fig. 11. Micrograph of the alloy aged at 560°C for 4 hr after thermo-

magnetic treatment at 640°C for 1 hr, Hc~160 Oe, showing the
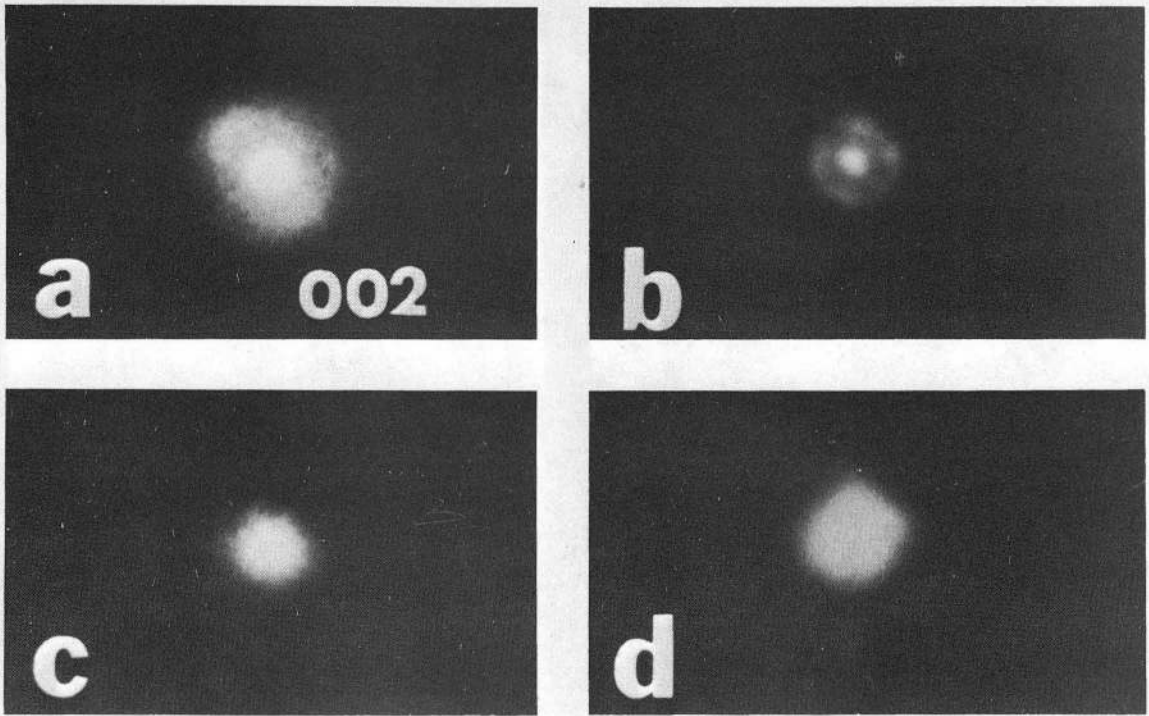
secondary decomposition.
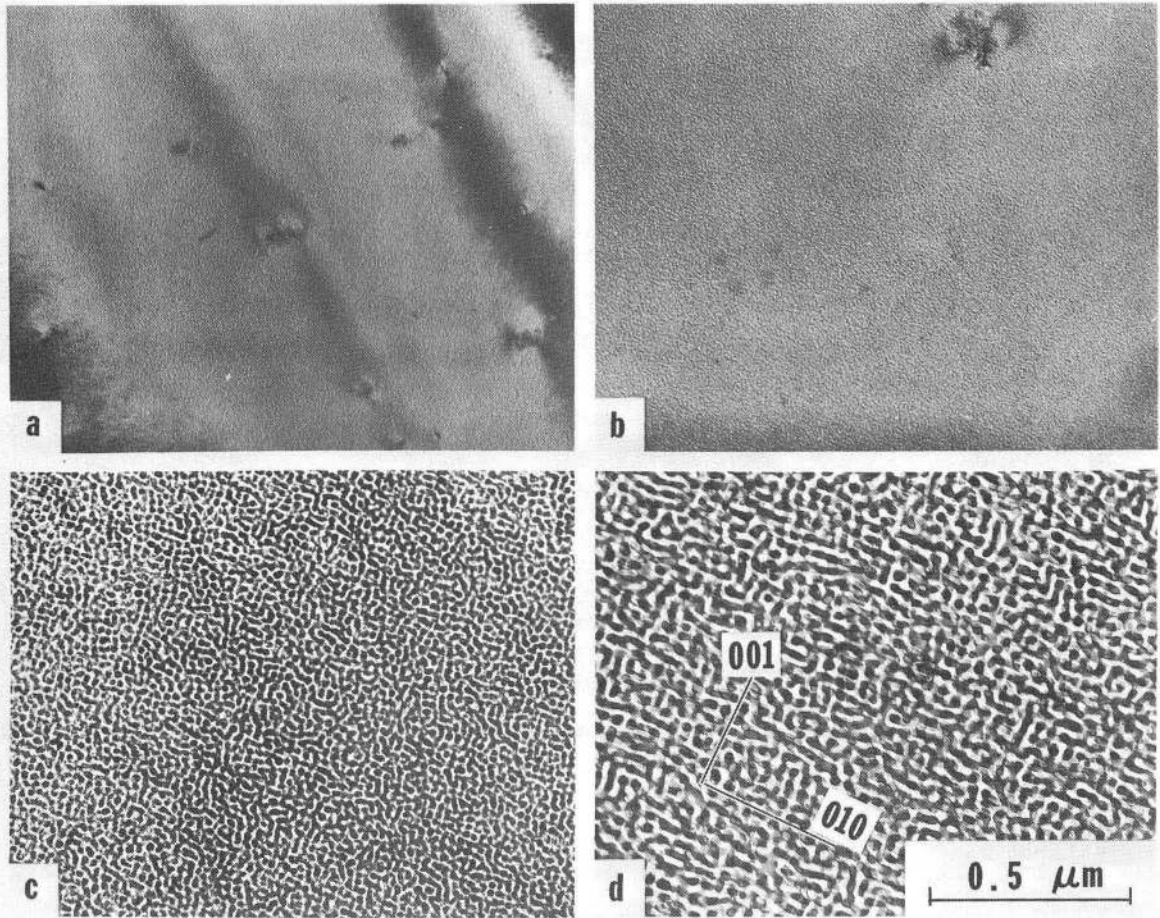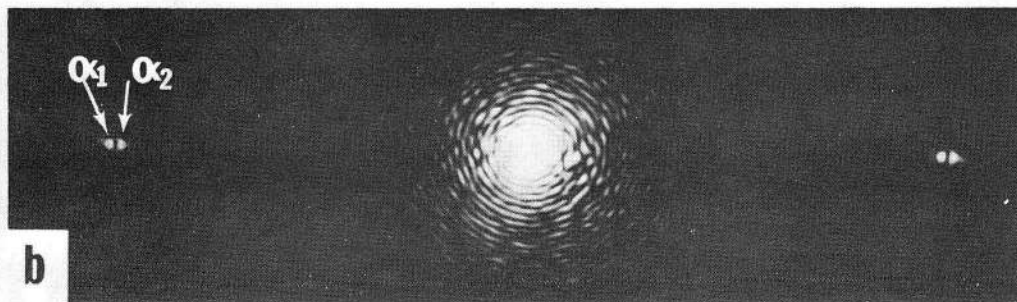
XBB 769-8660
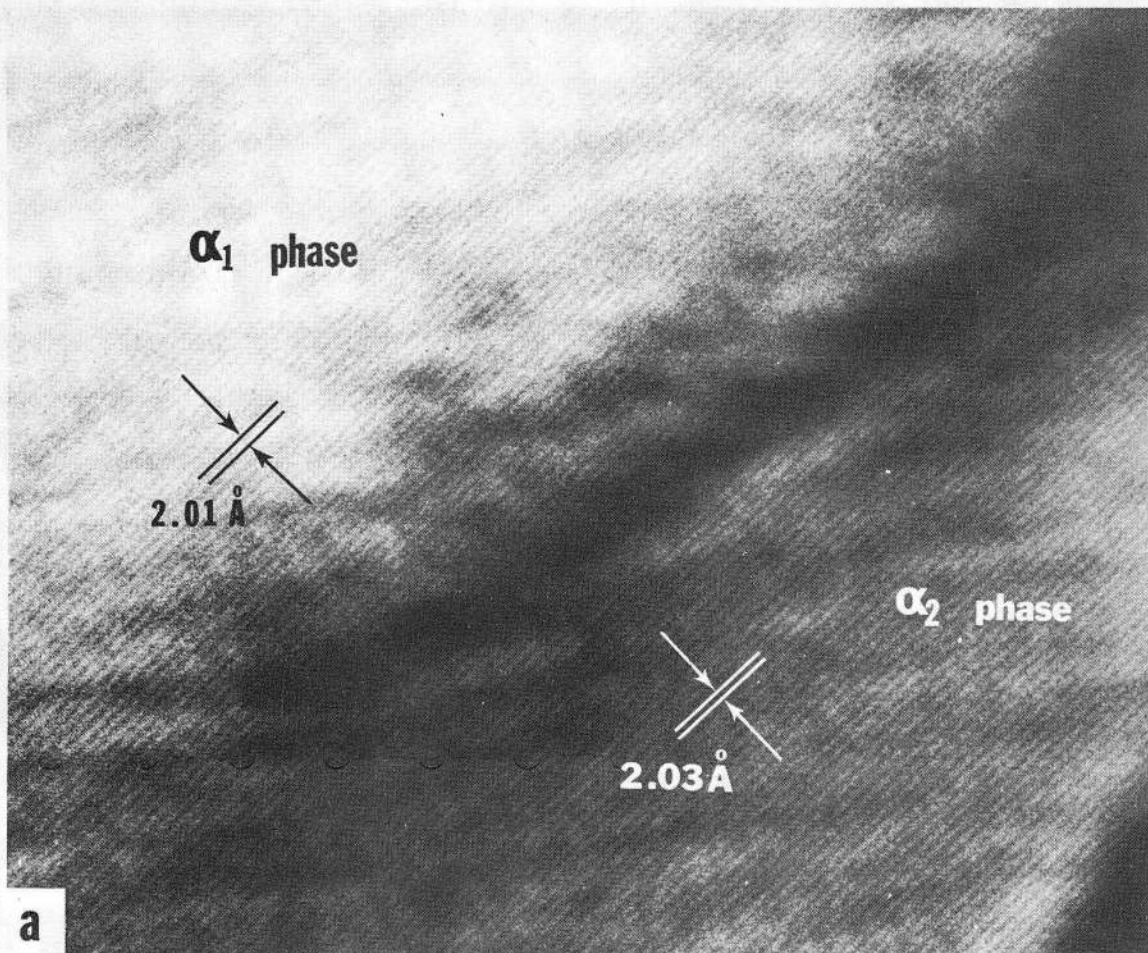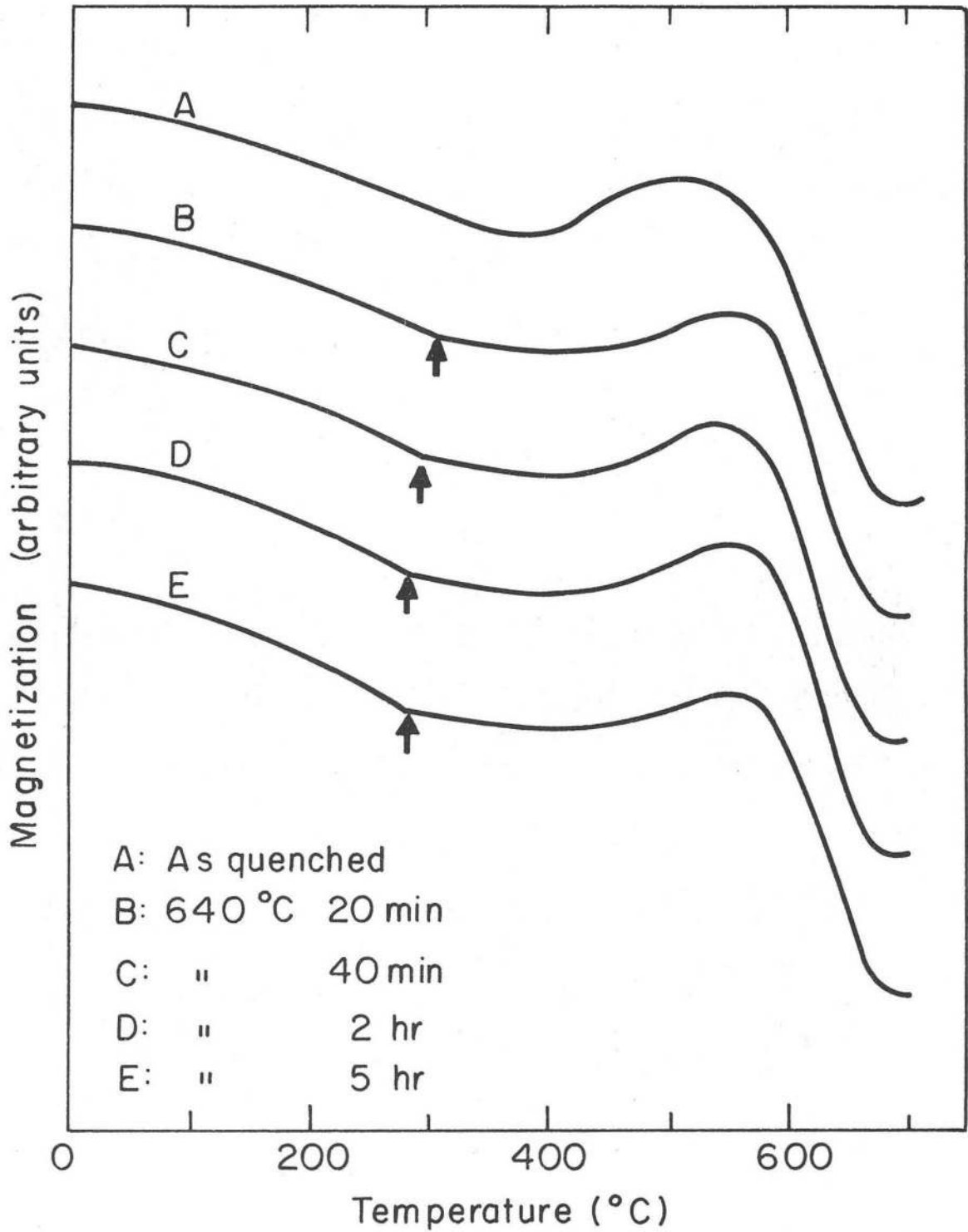
FIG. 1

FIG. 2

XBB-773-1698

XBB 778-8116

FIG. 3

FIG. 4

XBB 773-1699

a

α_1 phase

2.01 Å

α_2 phase

2.03Å

b

α_1 α_2

XBB 773-1892

FIG. 5

A: As quenched
B: 640 °C 20 min
C: " 40 min
D: " 2 hr
E: " 5 hr

XBL 7610-7638

FIG. 6

FIG. 7

XBL 7610-7640

2500 Å

XBB 760-11047

FIG. 8

FIG. 9

XBB 760-11044

FIG. 10

2000 Å

XBB 775-5209

FIG. 11